arXiv:1610.03250v3 [hep-ph] 17 Nov 2016

Searches for the FCNC couplings from top-Higgs associated production signal with $h \to \gamma\gamma$ at the LHC

Yao-Bei Liu[1*], Zhen-Jun Xiao[2†]

1. Henan Institute of Science and Technology, Xinxiang 453003, P.R.China

2. Department of Physics and Institute of Theoretical Physics, Nanjing Normal University, Nanjing 210023, P.R.China

Abstract

In this paper, we study the observability of the top-Higgs flavor changing neutral current (FCNC) tqh coupling through the process $pp \to qg \to t(\to \ell^+ b\nu)h(\to \gamma\gamma)$ at the Large Hadron Collider (LHC), where $\ell = e, \mu$. Our numerical results show that, in some parameter regions, the LHC may observe the above signals at the 5σ level. Otherwise, the branching ratios $Br(t \to uh)$ and $Br(t \to ch)$ can be respectively probed to 0.036% and 0.13% at 3σ level at 14 TeV LHC with the high integrated luminosity of 3000 fb^{-1}. On the other hand, studying the charge ratio for the lepton in top quark decay can be not only used to discriminate between signal and backgrounds, but also used to discriminate between tuh and tch couplings, for which anomalous single top production comes from the up initiated channel and charm initiated channel.

PACS numbers: 14.65.Ha,14.80.Bn,11.30.Hv

* E-mail: liuyaobei@sina.com

† E-mail: xiaozhenjun@njnu.edu.cn

I. INTRODUCTION

The discovery of a Higgs boson with a mass about 125 GeV is the undisputed highlight of Run-I of the CERN's Large Hadron Collider (LHC) [1, 2]. So far the measured couplings of the Higgs boson with fermions and gauge bosons are found to be in agreement with the predictions of the Standard Model (SM) [3, 4]. A major target of the future LHC programme is to study the intrinsic properties of the discovered Higgs boson. In view of the large top quark mass and the large number of top quarks produced at the LHC, it is attractive to investigate the anomalous flavor-changing neutral current (FCNC) top-Higgs couplings [5–13].

In the SM, the FCNC couplings in the top sector are strongly suppressed due to the Glashow-Iliopoulos-Maiani (GIM) mechanism [14], which can only occur at loop-level with the expected branching ratios of order about $10^{-15} - 10^{-12}$ [15, 16]. However, in many new physics (NP) models beyond the SM, such as the Minimal Supersymmetric Standard Model (MSSM) [17–21], Two-Higgs-Doublet Models (THDM) [22–26], Extra Dimensions (ED) [27], Little Higgs Models (LHT) [28], and the other miscellaneous models [29–33], some FCNC processes involving the top quark can be greatly enhanced by extending the flavor structures, which makes them potentially accessible at current and future high-energy colliders. Thus, any signal for top quark FCNC process at a measurable rate would be a robust evidence for NP. Since we do not know which type of NP models will be responsible for the possible deviation, it is better to study these processes with a model-independent method. So far, there are already many studies on the probe of the anomalous FCNC couplings in the top quark sector within model-independent method [34–40].

Recently, the ATLAS and CMS collaborations have set the upper limits of $Br(t \to qH) < 0.79\%$ [41] and $Br(t \to cH) < 0.56\%$ at 95% confidence level (C.L.) [42]. The production of the top pair ($t\bar{t}$) and associated top-Higgs (th) via FCNC couplings has been emphasized in the recent studies [43–54]. Especially, the author of [43] studied the anomalous production of th via the FCNC interaction of tqh at the LHC through the $h \to b\bar{b}$ channel including complete QCD next-to-leading order (NLO) corrections. The anomalous production of th at the LHC originating from FCNC interactions in tqg and tqh vertices has also been studied via the $h \to b\bar{b}$ decay channel [45]. Although the

branching ratio of Higgs diphoton decay channel is small, it has the advantages of good resolution on the Higgs mass and small QCD backgrounds. Thus in this paper, we mainly investigate the top-Higgs FCNC interactions through $pp \to th$ with the sequent decays $t \to W^+b \to \ell^+\nu b$ and $h \to \gamma\gamma$ at the LHC.

This paper is organized as follows. In Sec. II, we give a brief introduction to the anomalous FCNC tqh couplings and our selected production channel. In Sec. III, we discuss the observability of the top-Higgs FCNC couplings through the process $pp \to t(\to W^+b \to \ell^+\nu b)h(\to \gamma\gamma)$ at 14 TeV LHC. In Sec. IV, we discuss the leptonic charge ratio of the signal and backgrounds. Finally, we summarize our conclusions in Section. V.

II. CALCULATION FRAMEWORK

A. Top-Higgs FCNC couplings

In general, the effective Lagrangian describing the FCNC Yukawa interactions of a light up-type quark with the top quark and a Higgs boson can be written as [55]

$$\mathcal{L} = \lambda_{tuh}\bar{t}Hu + \lambda_{tch}\bar{t}Hc + h.c., \tag{1}$$

where the real coefficient λ_{tqh} $(q = u, c)$ denotes the strength of the top-Higgs FCNC coupling. At the leading order (LO) and the NLO, the decay widths of the dominant top quark decay mode $t \to Wb$ could be found in Ref. [56]. After neglecting all the light quark masses and assuming the dominant top decay width $t \to bW$, the branching ratio of $t \to qh$ can be approximately given by [44]:

$$Br(t \to qh) = \frac{\lambda_{tqH}^2}{\sqrt{2}m_t^2 G_F}\frac{(1-x_h^2)^2}{(1-x_W^2)^2(1+2x_W^2)}\kappa_{QCD} \simeq 0.58\lambda_{tqh}^2, \tag{2}$$

with the Fermi constant G_F, the top quark mass m_t, the W boson mass m_W, the Higgs mass m_h and $x_i = m_i/m_t$ $(i = W,\ h)$. Here the factor κ_{QCD} is the NLO QCD correction to $Br(t \to qh)$ and equals about 1.1 [57].

Currently, the stringent constraints on the anomalous FCNC couplings are set exploiting the experimental data of the ATLAS and CMS Collaborations [41, 42]. On the other hand, the low energy observables, such as $D^0 - \bar{D}^0$ mixing [58] and $Z \to c\bar{c}$ [59] can also be used to constrain the top quark flavor violation in the tqH vertex. With the 125 GeV

Higgs boson mass, upper limits of $Br(t \to cH) < 2.1 \times 10^{-3}$ have been obtained from the $Z \to c\bar{c}$ decay [50]. The author of [60] also derived model-independent constraints on the tcH and tuH couplings that arised from the bounds on hadronic electric dipole moments.

B. The production processes

At the LHC, the parton level signal process at the tree-level via the FCNC htq couplings can be expressed as

$$qg \to tH, \tag{3}$$

where q is u or c quark. The Feynman diagrams are shown in Fig. 1. Obviously, the conjugate process $\bar{t} + h$ production can also occur at the tree level.

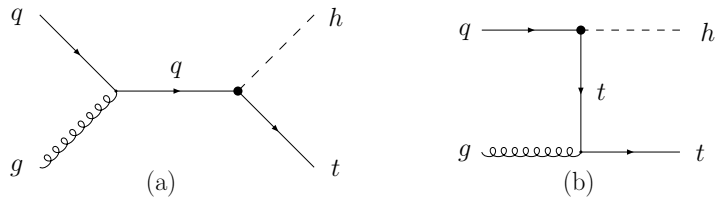

FIG. 1: The LO Feynman diagrams for th associated production at the LHC through FCNC top-Higgs interactions. Here $q = u, c$.

We first implement the tqH FCNC interactions by using the `FeynRules` package [61]. The LO cross section are computed using `MadGraph5-aMC@NLO` [62] with CTEQ6L parton distribution function (PDF) [63], setting the renormalization and factorization scales to be $\mu_R = \mu_F = \mu_0/2 = (m_t + m_h)/2$. In this work, we assume $\lambda_{tqh} \leq 0.1$ to satisfy the direct constraints from the ATLAS and CMS results [41, 42]. The SM input parameters

are taken as follows [64]:

$$m_H = 125 \text{ GeV}, \quad m_t = 173.21 \text{ GeV}, \quad m_W = 80.385 \text{ GeV}, \tag{4}$$
$$\alpha(m_Z) = 1/127.9, \quad \alpha_s(m_Z) = 0.1185, \quad G_F = 1.166370 \times 10^{-5} \text{ GeV}^{-2}.$$

In Fig. 2, we show the dependence of the cross sections σ_{th} and $\sigma_{\bar{t}h}$ on the top-Higgs FCNC couplings λ_{tqh} at 14 TeV LHC for different processes. From Fig. 2, we can see that the cross section of $ug \to th$ is larger than that for other processes. To be specific, when $\sqrt{s} = 14$ TeV and $\lambda_{tqh} = 0.1$, the production cross section σ is about 20 pb, which is roughly an order of magnitude larger than that for the conjugate process $\bar{u}g \to \bar{t}h$ due to the difference between the u-quark and $\bar{u}$-quark PDF of the proton. Thus, for a given center-of-mass (c.m.) energy and luminosity, more leptons will be observed than anti-leptons considering the leptonic top decays $t \to W^+(\to \ell^+\nu_\ell)b$ and $\bar{t} \to W^-(\to \ell^-\bar{\nu}_\ell)\bar{b}$. On the other hand, since the c-quark and $\bar{c}$-quark have the similar small PDF, the production rates of top and anti-top quarks from the processes of $gc(\bar{c}) \to ht(\bar{t})$ are almost the same

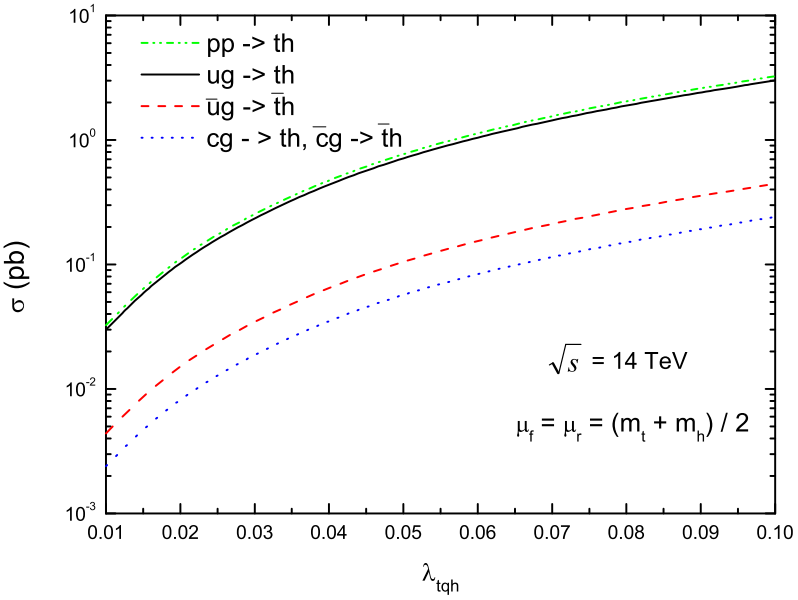

FIG. 2: The dependence of the cross sections σ at 14 TeV LHC on the top-Higgs FCNC couplings λ_{tqh}.

and smaller than that for the process $ug \to th$. This implies that the sensitivity to the coupling λ_{tuh} will be better than λ_{tch}.

III. SIGNAL AND DISCOVERY POTENTIALITY

In this section, we perform the Monte Carlo simulation and explore the sensitivity of 14 TeV LHC to the top-Higgs FCNC couplings through the channel,

$$pp \to t(\to W^+ b \to \ell^+ \nu b) h(\to \gamma\gamma), \tag{5}$$

where $\ell = e, \mu$. The Feynman diagram of production and decay chain is presented in Fig. 3.

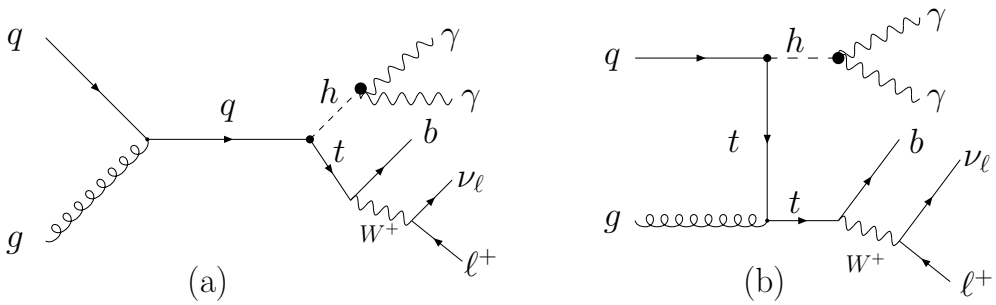

FIG. 3: The Feynman diagram for production of th including the decay chain with leptonic top quark decay and Higgs decay into diphoton.

Obviously, the signal is taken as the single top plus a Higgs boson followed by the leptonic top quark decay and the Higgs boson decay into two photons, which is characterized by two photons appearing as a narrow resonance centered around the Higgs boson mass. The main SM backgrounds which yield the identical final states to the signal are Whj, $Wj\gamma\gamma$ and $tj\gamma\gamma$, where j denotes non-bottom-quark jets. Besides, with fake photons due

to misidentified jets or electrons, the reducible backgrounds such as $Wjj\gamma$, $tjj\gamma$, $tj\gamma$, $t\bar{t}\gamma$, $t\bar{t}\gamma\gamma$ can be important as well. On the other hand, the SM thj, ZWh, W^+W^-h and $t\bar{t}h$ events can also be the sources of backgrounds for our signal. We have not included these backgrounds in the analysis due to very small cross sections. After including the branching ratios and applying the cuts, a negligible number of events will survive.

All of these signal and backgrounds events are generated at LO using `MadGraph5-aMC@NLO` with the CTEQ6L PDF. `PYTHIA` [65] is utilized for parton shower and hadronization. `Delphes` [66] is then employed to account for the detector simulations and `MadAnalysis5` [67] for analysis, where the (mis-)tagging efficiencies and fake rates are assumed to be their default values, which is formulated as a function of the transverse momentum and rapidity of the jets. When generating the parton level events, we assume $\mu_R = \mu_F$ to be the default event-by-event value. The anti-k_t algorithm [68] with the jet radius of 0.4 is used to reconstruct jets. The high order corrections for the dominant backgrounds are considered by including a k-factor, which is 1.12 for Whj [69] and 1.3 for $Wj\gamma\gamma$ [70, 71], respectively. Here it should be mentioned that the k-factor for the LO cross section of σ_{th} is chosen as 1.5 at the 14 TeV LHC [43]. In order to avoid the double-counting issue of jets originated from matrix element calculation and the parton shower, we apply the MLM-matching implemented in `MadGraph5-aMC@NLO` [72]. In practice, for the background events of Whj, we include both processes $pp \to Whj$ and $pp \to Whj + j$ to form an inclusive dataset, and similarly for other backgrounds.

In our simulation, we generate 10^6 events for the signals and backgrounds respectively. We first employ some basic cuts for the selection of events:

$$\begin{aligned} p_T^{j,b,\ell} &> 25 \text{ GeV}, \quad |\eta_{\rm j,b,\ell}| < 2.5, \\ \not{E}_T^{miss} &> 25 \text{ GeV}, \quad \Delta {\rm R}_{\rm ij} > 0.4 \ \ ({\rm i,j} = \ell, {\rm b, j}, \gamma). \end{aligned} \tag{6}$$

where p_T and η are the transverse momentum and the pseudo-rapidity of jets and leptons while $\not{E}_T^{miss}$ is the missing transverse momentum. $\Delta R = \sqrt{(\Delta\phi)^2 + (\Delta\eta)^2}$ is the particle separation with $\Delta\phi$ and $\Delta\eta$ being the separation in the azimuth angle and rapidity respectively. For the signal, we require exactly one charged lepton, one b-jet, two photons and missing energy in the final state. To trigger the signal events, $N(\ell) = 1$, $N(b) = 1$ and $N(j) < 2$ are applied, which can help to suppress the background events effectively, especially to the events with fake particles.

It should be mentioned that the $pp \to t\bar{t} \to thq$ process could also be considered as a source of top plus a Higgs boson if the light quark is missed by the detector. It has been shown that this additional contribution is very significant for detecting the λ_{tch} couplings due to the suppressed production cross section for the $cg \to th$ process [43]. Therefore, we also consider this process when discussing the tch couplings. In our calculation, the FCNC couplings are chosen to be $\lambda_{tuh} = 0.1$ and $\lambda_{tch} = 0.1$, which are allowed by the low-energy experiments [58, 59].

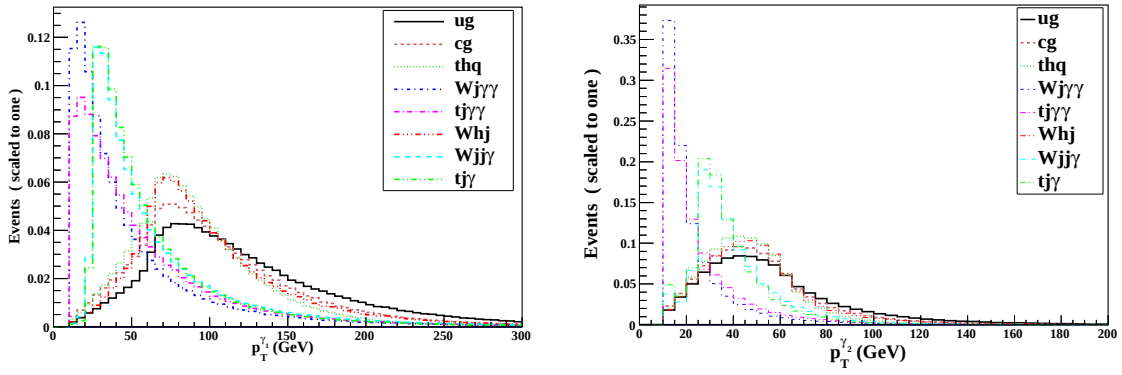

FIG. 4: Normalized distributions of transverse momentum $p_T^{\gamma 1}$ and $p_T^{\gamma 2}$ in the signals and backgrounds at 14 TeV LHC.

In Fig. 4, we show the transverse momentum distributions of two photons in the signal and backgrounds at 14 TeV LHC. Since the two photons in the signal and the resonant backgrounds come from the Higgs boson, they have the harder p_T spectrum than those in the non-resonant backgrounds. Thus, we can apply the cuts $p_T^{\gamma 1} > 55$ GeV and $p_T^{\gamma 2} > 25$ GeV to suppress the non-resonant backgrounds.

Since there are only one b jet and one lepton in the final states, it is easily to reconstruct the top quark transverse cluster mass, which is defined as

$$M_T^2 \equiv (\sqrt{(p_\ell + p_b)^2 + |\vec{p}_{T,\ell} + \vec{p}_{T,b}|^2} + |\vec{\not{p}}_T|)^2 - |\vec{p}_{T,\ell} + \vec{p}_{T,b} + \vec{\not{p}}_T|^2, \tag{7}$$

where $\vec{p}_{T,\ell}$ and $\vec{p}_{T,b}$ are the transverse momentums of the charged leptons and b-quark, respectively, and $\vec{\not{p}}_T$ is the missing transverse momentum determined by the negative sum of visible momenta in the transverse direction. In Fig. 5, we show the transverse mass

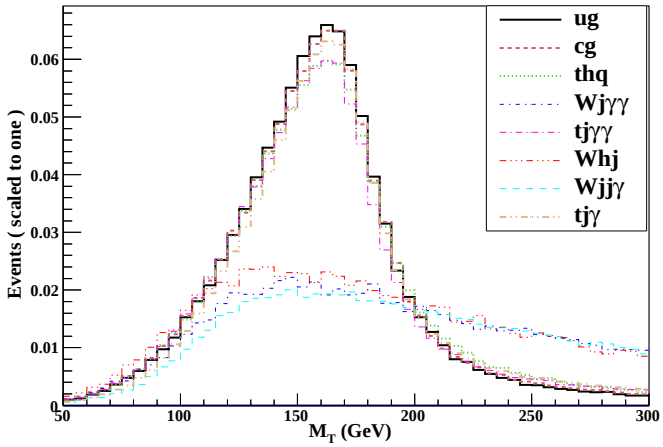

FIG. 5: Normalized transverse mass distribution for the $b\ell\not{E}_T$ system at 14 TeV LHC.

distribution for the $b\ell\not{E}_T$ system, which has been defined in the `MadAnalysis5` [73]. From this figure, we can see that the distributions of signal and backgrounds including top quark have peaks around the top quark mass. Therefore, we choose the transverse mass M_T cuts

$$120 \text{ GeV} < \text{M}_\text{T} < 190 \text{ GeV}. \tag{8}$$

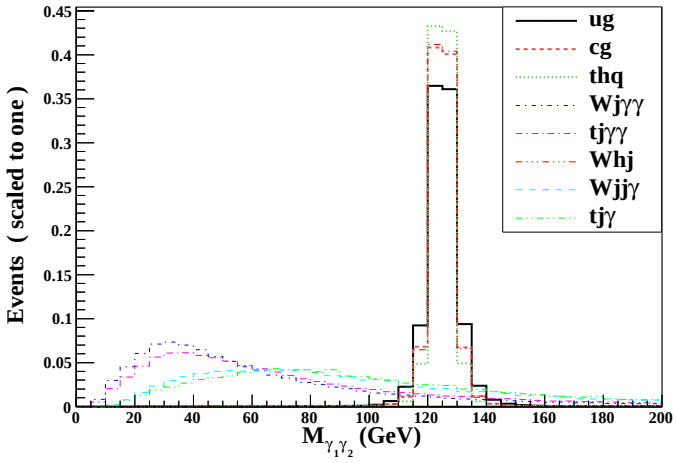

FIG. 6: Normalized invariant mass distribution of two photons at 14 TeV LHC.

Next we consider to utilize the invariant mass distributions to further suppress the background. Fig. 6 illustrates the normalized invariant mass distribution $M_{\gamma\gamma}$ of the signal and backgrounds. We can see that the signals and the resonant backgrounds including the Higgs boson have peaks around 125 GeV. Thus we can further reduce the non-resonant backgrounds by the following cut:

$$120 \text{ GeV} < \mathrm{M}_{\gamma_1\gamma_2} < 130 \text{ GeV}. \tag{9}$$

For a short summary, we list all the cut-based selections here:

- Basic cuts: $N(\ell) = 1$, $N(b) = 1$, $N(j) < 2$, $p_T^{j,b,\ell} > 25$ GeV, $|\eta_{j,b,\ell}| < 2.5$, $\not{E}_T^{miss} > 25$ GeV and $\Delta R_{i,j} > 0.4$ $(i, j = j, b, \ell, \gamma)$;
- Cut 1 means the basic cuts plus $p_T^{\gamma_1} > 55$ GeV, $p_T^{\gamma_2} > 25$ GeV;
- Cut 2 means Cut 1 plus $120 \text{ GeV} < \mathrm{M_T}(\ell^+\mathrm{b}\not{E}_{\mathrm{T}}^{\mathrm{miss}}) < 190$ GeV.
- Cut 3 means Cut 2 plus requiring the invariant mass of the diphoton pair to be in the range $m_h \pm 5$ GeV.

The cross sections of the signal and backgrounds after imposing the cuts are summarized in Table I. For the numbers of the cross sections as listed in the Table I, the FCNC couplings are chosen to be $\lambda_{tuh} = 0.1$ and $\lambda_{tch} = 0.1$. From Table I, we can see that after all these cuts, all the backgrounds are suppressed efficiently and the total production cross section for the backgrounds is about 9.4×10^{-4} fb. The final production cross sections of thj, $t\bar{t}\gamma$ and $t\bar{t}\gamma\gamma$ are all at the level of 10^{-6} fb and thus they can be safely neglected. However, the cross section of the process $pp \to t\bar{t} \to thq$ is comparable to that of $cg \to th$. As stated before, we should include these two processes when discussing the tch couplings.

In order to illustrate excluded detection potential regions of anomalous couplings to reach a given statistical significance, we define the statistical significance (SS) as [74]:

$$SS = \sqrt{2L[(S+B)\ln(1+\frac{S}{B}) - S]}, \tag{10}$$

where S and B are the signal and background cross sections and L is the integrated luminosity. Here we define the discovery significance as $SS = 5$ and exclusion limits as $SS = 3$.

TABLE I: The cut flow of the cross sections (in 10^{-3} fb) for the signal and backgrounds at the 14 TeV LHC. The FCNC couplings are chosen to be $\lambda_{tuh} = 0.1$ and $\lambda_{tch} = 0.1$.

Cuts	ug	cg	$t\bar{t} \to thq$	Whj	$Wj\gamma\gamma$	$tj\gamma\gamma$	$Wjj\gamma$	$tj\gamma$	$tjj\gamma$
Basic cuts	69.2	10.1	9.6	0.57	270.5	3.6	2215	132	425
Cut 1	56.5	7.45	7.5	0.41	35.5	5.3	16.8	5.54	2.72
Cut 2	45.2	5.96	5.33	0.14	6.03	3.1	1.68	4.05	8.98
Cut 3	33.9	4.95	4.53	0.12	0.54	0.015	0.09	0.13	0.05

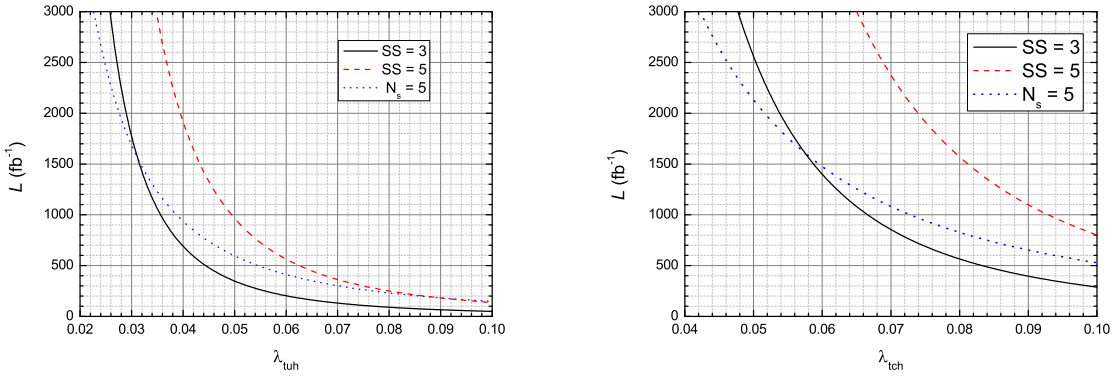

FIG. 7: 3σ and 5σ contour plots for the signal in $L - \lambda_{tuh}$ (left) and $L - \lambda_{tch}$ (right) planes at 14 TeV LHC. The dotted line denotes the required minimum number of signal events $N_s = 5$.

In Fig. 7, we plot the excluded 3σ and 5σ discovery reaches in the plane of the integrated luminosity and the coupling parameter λ_{tqh}. To observe the signal at the LHC, we here also require the minimum 5 events for the signal. From Fig. 7, we can see that the 5σ C.L. discovery sensitivity of λ_{tuh} is 0.062, 0.049 and 0.034 when the integrated luminosity is 500, 1000 and 3000 fb^{-1}, respectively. For the thc couplings, the 5σ C.L. discovery sensitivity of λ_{tch} is 0.065 when the integrated luminosity is 3000 fb^{-1}.

If no signal is observed, it means that the FCNC tqh couplings can not be too large. The upper limits on the FCNC couplings λ_{tuh} and λ_{tch} can be respectively probed to 0.025 and 0.047 with $L = 3000$ fb^{-1}. These limits can be converted to the 3σ C.L. upper limits on the branching ratio $Br(t \to uh) = 0.036\%$ and $Br(t \to ch) = 0.13\%$, respectively.

Compared with other phenomenological studies, we can see that our result is comparable with the sensitivity limits of LHC as $Br(t \to uh) < 5 \times 10^{-4}$ via multi-leptons channel with an integrated luminosity of 3000 fb^{-1} at $\sqrt{s} = 14$ TeV [46].

IV. CHARGE RATIO FOR SIGNAL AND BACKGROUNDS

As we discussed in Sec. II, the useful handle on tagging th production in searches with leptonic decays of top quark is the enhanced abundance of positively charged leptons. Due to the difference between the u-quark and $\bar{u}$-quark PDF, the cross sections of th and $\bar{t}h$ are different for the processes $u(\bar{u})g \to t(\bar{t})h$ at the LHC. Since the efficiencies of lepton selection and fake charged lepton contamination are almost independent of charge, the top (anti-top) asymmetry can be directly translated in a corresponding lepton charge asymmetry.

TABLE II: The values of R for the signal and backgrounds at the 14 TeV LHC.

Process	$ug(pp) \to th$			cg	Whj	$Wj\gamma\gamma$	$tj\gamma\gamma$	$Wjj\gamma$	$tj\gamma$
	$\mu_0/2$	μ_0	$2\mu_0$						
R	6.76(4.74)	6.75(4.67)	6.75(4.64)	1.0	1.57	1.17	1.59	1.17	1.45

In this analysis, we define a ratio $R = N^+/N^-$ as the number of events with positive charged lepton to the number of events with negative charge. For the signal and relevant backgrounds, the values of R are listed in Table II at 14 TeV LHC with the same basic cuts. Here we present three typical renormalization scale and factorization scale as $\mu_R = \mu_F = \mu_0/2$, μ_0 and $2\mu_0$, respectively. One can see that, for $\lambda_{tch} = \lambda_{tuh} = 0.1$, the value of the charge ratio for the signal is insensitive to the renormalization and factorization scales, and it is significantly larger than that for the SM backgrounds. In Fig. 8 we show the dependence of the charge ratio R for the process $pp \to th$ on the various of ratio values $\lambda_{tuh}/\lambda_{tch}$ at the 14 TeV LHC. One can see that for the case of $\lambda_{tuh} \gg \lambda_{tch}$, the contribution from the tuh vertex can enhance the charge ratio, while for the case of $\lambda_{tuh} \ll \lambda_{tch}$, the contribution from the tch vertex can significantly dilute the ratio. Therefore, studying the charged ratio for lepton can be not only used to discriminate

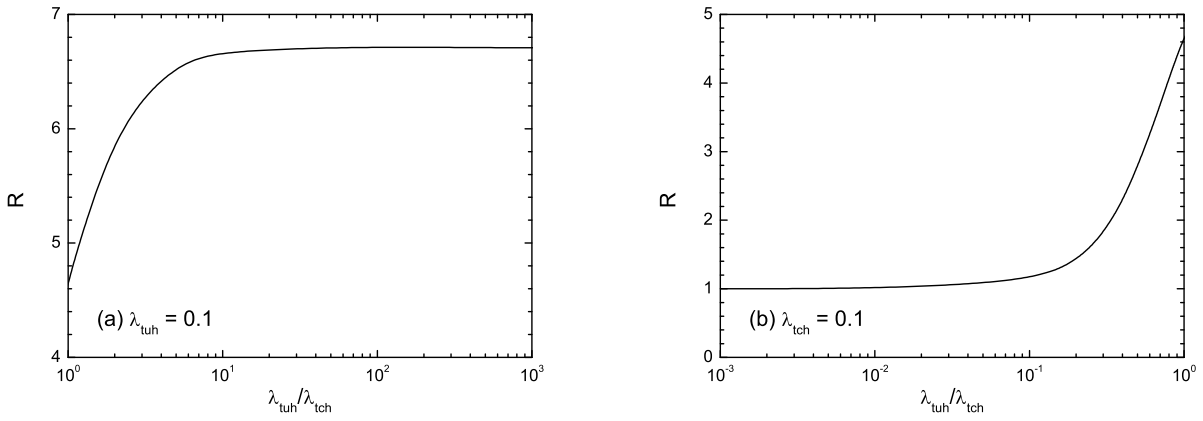

FIG. 8: The dependence of the charge ratio R for the process $pp \to th$ on the various of ratio values $\lambda_{tuh}/\lambda_{tch}$ at the 14 TeV LHC with (a) $\lambda_{tuh} = 0.1$ and (b) $\lambda_{tch} = 0.1$.

between signal and backgrounds, but also used to determine that the signal comes from the up initiated production channel and charm initiated production channel.

V. CONCLUSION

In the work, we investigated the process $pp \to th$ induced by the top-Higgs FCNC couplings at the LHC. We also studied the observability of top-Higgs FCNC couplings through the process $pp \to t(\to W^+b \to \ell^+\nu b)h(\to \gamma\gamma)$ and proposed the charge ratio of signal and backgrounds of the charge lepton. From our numerical calculations and the phenomenological analysis we found the following points:

1. The cross section of $pp \to ug \to th$ is larger than that for other process due to the larger PDF of the u-quark, which means that the sensitivity to the FCNC coupling λ_{tuh} is better than λ_{tch}.

2. We further studied the observability of top-Higgs FCNC couplings through the process $pp \to t(\to W^+b \to \ell^+\nu b)h(\to \gamma\gamma)$ and found that in some parameter regions, the LHC may observe the above signals at the 5σ confidence level. Otherwise, the branching ratios $Br(t \to uh)$ and $Br(t \to ch)$ can be respectively probed to 0.036% and 0.13% at 3σ level at 14 TeV LHC with the integrated luminosity of 3000 fb^{-1}.

3. The charge ratio for the lepton in the signal is significantly larger than that for the SM backgrounds, which can be not only used to discriminate between signal and backgrounds, but also used to determine that the signal comes from the up initiated production channel and charm initiated production channel.

Acknowledgments

This work is supported by the National Natural Science Foundation of China under the Grant No.11235005, the Joint Funds of the National Natural Science Foundation of China (U1304112) and the Foundation of He'nan Educational Committee (2015GGJS-059).

---

[1] ATLAS Collaboration, **Phys. Lett. B 716** (2012) 1.

[2] CMS Collaboration, **Phys. Lett. B 716** (2012) 30.

[3] ATLAS Collaboration, **Phys. Lett. B 726** (2013) 88.

[4] V. Khachatryan *et al.*, [CMS Collaboration], **Eur. Phys. J. C** 75 (2015) 212; V. Khachatryan *et al.*, [CMS Collaboration], **Eur. Phys. J. C** 75 (2015) 251.

[5] W. Bernreuther, **J. Phys. G 35** (2008) 083001; J. A. Aguilar-Saavedra, **Nucl. Phys. B 812** (2009) 181; J. A. Aguilar-Saavedra, **Nucl. Phys. B 821** (2009) 215.

[6] C. S. Li, H. T. Li and D. Y. Shao, **Chin. Sci. Bull. 59** (2014) 3709; C. Zhang and S. Willenbrock, **Phys. Rev. D 83** (2011) 034006; C. Zhang and S. Willenbrock, **Nuovo Cim. C033** (2010) 285, arXiv:1008.3155 [hep-ph].

[7] M. Beneke, I. Efthymiopoulos, M. L. Mangano *et al.*, hep-ph/0003033; T. M. P. Tait and C.-P. Yuan, **Phys. Rev. D 63** (2000) 014018; F. Maltoni, K. Paul, T. Stelzer and S. Willenbrock, **Phys. Rev. D 64** (2001) 094023.

[8] D. Chakraborty, J. Konigsberg and D. L. Rainwater, **Ann. Rev. Nucl. Part. Sci. 53** (2003) 301; E. W. N. Glover, F. del Aguila, J. A. Aguilar-Saavedra *et al.*, **Acta Phys. Polon. B 35** (2004) 2671; T. Han, **Int. J. Mod. Phys. A 23** (2008) 4107.

[9] S. Biswas, E. Gabrielli and B. Mele, **JHEP 1301** (2013) 088; S. Biswas, E. Gabrielli, F. Margaroli and B. Mele, **JHEP 1307** (2013) 073.

[10] C. Englert and E. Re, **Phys. Rev. D 89** (2014) 073020; J. Ellis, D. S. Hwang, K. Sakurai and M. Takeuchi, **JHEP 1404** (2014) 004; J. Chang, K. Cheung, J. S. Lee and C.-T. Lu, **JHEP 1405** (2014) 062.

[11] A. Kobakhidze, L. Wu and J. Yue, **JHEP 1410** (2014) 100; J. Yue, **Phys. Lett. B 744** (2015) 131.

[12] E. L. Berger, Q.-H. Cao, C.-R. Chen, C. S. Li, H. Zhang, **Phys. Rev. Lett. 106** (2011) 201801; H. Hesari, H. Khanpour, M. K. Yanehsari and M. M. Najafabadi, **Adv. High Energy Phys. 2014** (2014) 476490; H. Khanpour, S. Khatibi, M. K. Yanehsari and M. M. Najafabadi, arXiv:1408.2090 [hep-ph].

[13] Y.-C. Guo, C.-X. Yue and S. Yang, **Eur. Phys. J. C 76** (2016) 596.

[14] S. L. Glashow, J. Iliopoulos and L. Maiani, **Phys. Rev. D 2** (1970) 1285.

[15] G. Eilam, J. L. Hewett, A. Soni, **Phys. Rev. D 44** (1991) 1473; B. Mele, S. Petrarca, A. Soddu, **Phys. Lett. B 435** (1998) 401.

[16] A. Cordero-Cid, J. M. Hernandez, G. Tavarses-Velasco, J. J. Toscano, **Phys. Rev. D 73** (2006) 094005; G. Eilam, M. Frank, I. Turan, **Phys. Rev. D 73** (2006) 053011; J. A. Aguilar-Saavedra, **Acta Phys. Polon. B 35** (2004) 2695.

[17] C. S. Li, R. J. Oakes and J. M. Yang, **Phys. Rev. D 49** (1994) 293; J. M. Yang and C. S. Li, **Phys. Rev. D 49** (1994) 3412; J. M. Yang, B.-L. Young and X. Zhang, **Phys. Rev. D 58** (1998) 055001; J. Guasch and J. Sola, **Nucl. Phys. B 562** (1999) 3.

[18] G. Eilam, T. Han, J. M. Yang, X. Zhang, **Phys. Lett. B 510** (2001) 227; J. L. Diaz-Cruz, H.-J. He, C.-P. Yuan **Phys. Lett. B 530** (2002) 179; J. Cao, Z. Xiong and J. M. Yang, **Nucl. Phys. B 651** (2003) 87; M. Frank and I. Turan, **Phys. Rev. D 72** (2005) 035008; S. Bejar, J. Guasch and J. Sola, **JHEP 0510** (2005) 113.

[19] M. Frank and I. Turan, **Phys. Rev. D** 74 (2006) 073014; J. J. Cao, G. Eilam, M. Frank, K. Hikasa, G. L. Liu, I. Turan, J. M. Yang, **Phys. Rev. D 75** (2007) 075021; S. Bejar, J. Guasch, D. Lopez-Val and J. Sola, **Phys. Lett. B 668** (2008) 364.

[20] Z. -X. Heng, G. -R. Lu, L. Wu and J. M. Yang, **Phys. Rev. D 79** (2009) 094029; J. Cao, Z. Heng, L. Wu and J. M. Yang, **Phys. Rev. D 79** (2009) 054003; J. Cao, C. Han, L. Wu, J. M. Yang and M. Zhang, **Eur. Phys. J. C 74** (2014) 3058; T. -J. Gao, T. -F. Feng, F. Sun, H. -B. Zhang and S. -M. Zhao, **Chin. Phys. C 39** (2015) 073101.

[21] C. Balazs, H.-J. He, C.-P. Yuan, **Phys. Rev. D 60** (1999) 114001; H.-J. He, S. Kanemura, C.-P. Yuan, **Phys. Rev. D 68** (2003) 075010.

[22] T.P. Cheng and M. Sher, **Phys. Rev. D 35** (1987) 3484; J. L. Diaz-Cruz, R. Martinez, M. A Perez, A. Rosado, **Phys. Rev. D 41** (1990) 891; S. Bar-Shalom, G. Eilam, A. Soni, J. Wudka, **Phys. Rev. Lett. 79** (1997) 1217; W. S. Hou, G.-L. Lin and C.-Y. Ma, **Phys. Rev. D 56** (1997) 7434; D. Atwood, L. Reina and A. Soni, **Phys. Rev. D 55** (1997) 3156.

[23] S. Bejar, J. Guasch and J. Sola, **Nucl. Phys. B 600** (2001) 21; E. O. Iltan and I. Turan **Phys. Rev. D 67** (2003) 015004; A. Arhrib, K. Cheung, C. W. Chiang and T. C. Yuan, **Phys. Rev. D 73** (2006) 075015.

[24] T. Han and R. Ruiz, **Phys. Rev. D 89** (2014) 074045; K.-F. Chen, W.-S. Hou, C. Kao and M. Kohda, **Phys. Lett. B 725** (2013) 378; C. Kao, H.-Y. Cheng, W.-S. Hou and J. Sayre, **Phys. Lett. B 716** (2012) 225.

[25] R. Gaitan, R. Martinez and J. H. M. de Oca, arXiv:1503.04391 [hep-ph]; G. Abbas, A. Celis, X.-Q. Li, J. Lu and A. Pich, **JHEP 1506** (2015) 005; B. Altunkaynak, W.-S. Hou, C. Kao, M. Kohda and B. McCoy, **Phys. Lett. B 751** (2015) 135; F. J. Botella, G. C. Branco, M. Nebot, M. N. Rebelo, **Eur. Phys. J. C 76** (2016) 161.

[26] H.-J. He, S. Kanemura, C.-P. Yuan, **Phys. Rev. Lett. 89** (2002) 101803; H.-J. He and C.-P. Yuan, **Phys. Rev. Lett. 83** (1999) 28.

[27] K. Agashe, G. Perez, A. Soni, **Phys. Rev. D 75** (2007) 015002.

[28] B. Yang, N. Liu and J. Han, **Phys. Rev. D 89** (2014) 034020;

[29] F. del Aguila, J. A. Aguilar-Saavedra, R. Miquel, **Phys. Rev. Lett. 82** (1999) 1628; J. A. Aguilar-Saavedra, B. M. Nobre, **Phys. Lett. B 553** (2003) 251; J. Cao, K. Hikasa, L. Wang, L. Wu and J. M. Yang, **Phys. Rev. D 85** (2012) 014025.

[30] C. -X. Yue, S. -Y. Cao and Q. -G. Zeng, **JHEP 1404** (2014) 170; C. Han, N. Liu, L. Wu and J. M. Yang, **Phys. Lett. B 714** (2012) 295; J. Cao, L. Wu and J. M. Yang, **Phys. Rev. D 83** (2011) 034024.

[31] J. Drobnak, S. Fajfer and J. F. Kamenik, **JHEP 0903** (2009) 077; A. Azatov, M. Toharia and L. Zhu, **Phys. Rev. D 80** (2009) 035016; K. Agashe and R. Contino, **Phys. Rev. D 80** (2009) 075016; G.-R. Lu and L. Wu, **Chin. Phys. Lett. 27** (2010) 031401.

[32] A. Azatov, G. Panico, G. Perez and Y. Soreq, **JHEP 1412** (2014) 082; J. Cao, L. Wang, L. Wu and J. M. Yang, **Phys. Rev. D 84** (2011) 074001; J. Cao, Z. Heng, L. Wu and J. M. Yang, **Phys. Rev. D 81** (2010) 014016;

[33] H.-J. He, T.M.P. Tait, C.-P. Yuan, **Phys. Rev. D 62** (2000) 011702.

[34] J. A. Aguilar-Saavedra, **Acta Phys. Polon. B 35** (2004) 2695; J. M. Yang, **Annals Phys. 316** (2005) 529; F. Larios, R. Martinez, M. A. Perez, **Int. J. Mod. Phys. A 21** (2006) 3473; P. M. Ferreira, R. B. Guedes and R. Santos, **Phys. Rev. D 77** (2008) 114008.

[35] N. Craig, J. A. Evans, R. Gray *et al.*, **Phys. Rev. D 86** (2012) 075002.

[36] E. Yazgan [ATLAS and CDF and CMS and D0 Collaborations], arXiv:1312.5435 [hep-ex].

[37] G. Aad *et al.*, [ATLAS Collaboration], **Phys. Lett. B 712** (2012) 351; G. Aad *et al.*, [ATLAS Collaboration], **Eur. Phys. J. C 76** (2016) 55.

[38] V. Khachatryan *et al.*, [CMS Collaboration], **JHEP 1604** (2016) 035.

[39] C. Degrande, F. Maltoni, J. Wang, C. Zhang, **Phys. Rev. D 91** (2015) 034024; G. Durieux, F. Maltoni, C. Zhang, **Phys. Rev. D 91** (2015) 074017.

[40] V. Cirigliano, W. Dekens, J. de Vries, E. Mereghetti, **Phys. Rev. D 94** (2016) 034031.

[41] G. Aad *et al.* [ATLAS Collaboration], **JHEP 1406** (2014) 008.

[42] [CMS Collaboration], CMS-PAS-HIG-13-034 (2014).

[43] Y. Wang, F. P. Huang, C. S. Li, B. H. Li, D. Y. Shao, J. Wang, **Phys. Rev. D 86** (2012) 094014.

[44] A. Greljo, J. F. Kamenik and J. Kopp, **JHEP 1407** (2014) 046.

[45] S. Khatibi and M. M. Najafabadi, **Phys. Rev. D 89** (2014) 054011.

[46] K. Agashe *et al.*, [Top Quark Working Group Collaboration], arXiv:1311.2028 [hep-ph].

[47] Lei Wu, **JHEP** 1502 (2015) 061.

[48] W. Liu, H. Sun, X. Wang, and X. Luo, **Phys. Rev. D 92** (2015) 074015.

[49] H. Sun, arXiv:1602.04670 [hep-ph].

[50] H. Hesari, H. Khanpour and M. M. Najafabadi, **Phys. Rev. D 92** (2015) 113012.

[51] D. Atwood, S. K. Gupta and A. Soni, **JHEP 1410** (2014) 57.

[52] D. Lopez-Val, J. Guasch and J. Sola, **JHEP 0712** (2007) 054.

[53] J. A. Aguilar-Saavedra and G. C. Branco, **Phys. Lett. B 495** (2000) 347.

[54] Y.-B. Liu and Z.-J. Xiao, **Phys. Rev. D 94** (2016) 054018.

[55] C. Degrande, J.-M. Gerard, C. Grojean, F. Maltoni, G. Servant, **Phys. Lett. B 703** (2011) 306.

[56] C. S. Li, R. J. Oakes and T. C. Yuan, **Phys. Rev. D 43** (1991) 3759.

[57] J. J. Zhang, C. S. Li, J. Gao, H. Zhang, Z. Li, C. -P. Yuan and T. -C. Yuan, **Phys. Rev. Lett. 102** (2009) 072001; J. Drobnak, S. Fajfer and J. F. Kamenik, **Phys. Rev. Lett. 104** (2010) 252001; C. Zhang and F. Maltoni, **Phys. Rev. D 88** (2013) 054005.

[58] J. I. Aranda, A. Cordero-Cid, F. Ramirez-Zavaleta, J. J. Toscano, E. S. Tututi, **Phys. Rev. D 81** (2010) 077701.

[59] F. Larios, R. Martinez and M. A. Perez, **Phys. Rev. D 72** (2005) 057504.

[60] M. Gorbahn, U. Haisch, **JHEP 1406** (2014) 033.

[61] A. Alloul, N. D. Christensen, C. Degrande *et al.*, **Comput. Phys. Commum. 185** (2014) 2250.

[62] J. Alwall, M. Herquet, F. Maltoni *et al.*, **JHEP 1106** (2011) 128; J. Alwall, R. Frederix, S. Frixione *et al.*, **JHEP 1407** (2014) 079.

[63] J. Pumplin, A. Belyaev, J. Huston, D. Stump, W. K. Tung, **JHEP 0602** (2006) 032.

[64] K. A. Olive *et al.*, [Particle Data Group], **Chin. Phys. C 38** (2014) 090001.

[65] T. Sjostrand, S. Mrenna and P. Z. Skands, **JHEP 0605** (2006) 026.

[66] J. de Favereau *et al.*, [DELPHES 3 Collaboration], **JHEP 1402** (2014) 057.

[67] E. Conte, B. Fuks and G. Serret, **Comput. Phys. Commum. 184** (2013) 222.

[68] M. Cacciari, G. P. Salam and G. Soyez, **JHEP 0804** (2008) 063.

[69] J. J. Su, W.-G. Ma, R.-Y. Zhang, L. Guo, **Phys. Rev. D 81** (2010) 114037.

[70] F. Campanario, C. Englert, M. Rauch, D. Zeppenfeld, **Phys. Lett. B 704** (2011) 515.

[71] J. Alwall, R. Frederix, S. Frixione *et al.*, **JHEP 1407** (2014) 079.

[72] R. Frederix, S. Frixione, **JHEP 1212** (2012) 061.

[73] E. Conte, B. Dumont, B. Fuks and C. Wymant, **Eur. Phys. J. C 74** (2014) 3103.

[74] G. Cowan, K. Cranmer, E. Gross, and O. Vitells, **Eur. Phys. J. C 71** (2011) 1554 [Erratum-ibid. C **73** (2013) 2501] [arXiv:1007.1727 [physics.data-an]].